Available online at www.sciencedirect.com

ScienceDirect

Solid Earth Sciences 10 (2025) 100260

www.elsevier.com/locate/SESCI

Quantifying CO_2 in apatite by multiple unpolarized transmission FTIR analyses

Zhide Pu [a,b], Zhuoran Zhang [a,b], Xinjian Bao [a,b], Weiran Li [c], Xi Liu [a,b,*]

[a] Key Laboratory of Orogenic Belts and Crustal Evolution, Ministry of Education of China, Beijing 100871, China
[b] School of Earth and Space Sciences, Peking University, Beijing 100871, China
[c] Department of Earth Sciences, The University of Hong Kong, Pokfulam Road, China

Received 5 July 2025; revised 2 August 2025; accepted 5 August 2025
Available online ■ ■ ■

Abstract

CO_2 is a key volatile component in various fluids and magmas, and apatite is an ideal mineral for constraining the abundance, distribution and behavior of CO_2 in different materials of the Solar System. In sharp contrast to water, CO_2 in apatites has not been routinely investigated mainly due to lacking user-friendly analytical technique. Here we have developed a user-friendly analytical technique. By a Durango apatite crystal with a CO_2 content of ~277 (44) wt ppm, we performed 17 successful unpolarized transmission FTIR analyses on its randomly-selected fragments with unknown orientations. These analyses well reproduced the CO_2 content, attaining a relative difference of ~9 % only. Simple calculations carried out with this dataset suggest that as the number of the analyses increases from one, the accuracy of the result nonlinearly increases, being very fast at the first few analyses and much slower afterwards. Consequently, there are different minimum numbers of the analyses to meet different degrees of accuracy which may be required by different studies: it is highly unlikely to reach a result of any good by conducting one analysis only, but generally possible to arrive at a result with acceptable accuracy by performing two or three analyses, and almost certain to obtain a good result with high accuracy by collecting four or five analyses. If 10 or more analyses are possible, the accuracy of the result can be exceedingly high, with an absolute relative difference of < ~10 %. With this user-friendly new method employing multiple unpolarized transmission FTIR analyses on randomly oriented crystals, quantifying CO_2 in tiny apatite grains in different terrestrial and extraterrestrial materials can be readily actualized.

Keywords: Accuracy; Apatite; CO_2 concentration; Unpolarized transmission FTIR

1. Introduction

Of a small fraction but with a wide occurrence in different types of rocks of the Earth, the Moon, the Mars and other planets in the Solar System, apatite is an ideal mineral for probing their fluids/magmas' compositions, behaviors, and influences on their origins and evolutions (e.g., Steele and Smith, 1982; Ebihara and Honda, 1987; Nadeau et al., 1999; Greenwood et al., 2008; Boyce et al., 2010; McCubbin et al., 2015; Ge et al., 2024). Typical natural apatite is compositionally of $Ca_5(PO_4)_3(F,OH,Cl)$, with the volatile components F, OH and Cl hosted in its *c*-axis channel (Hughes et al., 1989). Indeed, these volatiles and their isotopes in apatites have been frequently characterized, and the data have been routinely used to constrain the abundances of volatiles like water in the fluids and magmas, to probe the origins and distributions of volatiles in the interiors of the terrestrial and extraterrestrial planets, and even to explore the early history of the Solar System (Greenwood et al., 2008; Boyce et al., 2010; McCubbin et al., 2010; Hu et al., 2014, 2021; Shang et al., 2022; He et al., 2025).

Apatite can also host significant quantities of volatile C (Fig. 1; Pan and Fleet, 2002; Piccoli and Candela, 2002), which often appears as carbonate either replacing the

* Corresponding author. Key Laboratory of Orogenic Belts and Crustal Evolution, Ministry of Education of China, Beijing 100871, China.
E-mail address: xi.liu@pku.edu.cn (X. Liu).

https://doi.org/10.1016/j.sesci.2025.100260

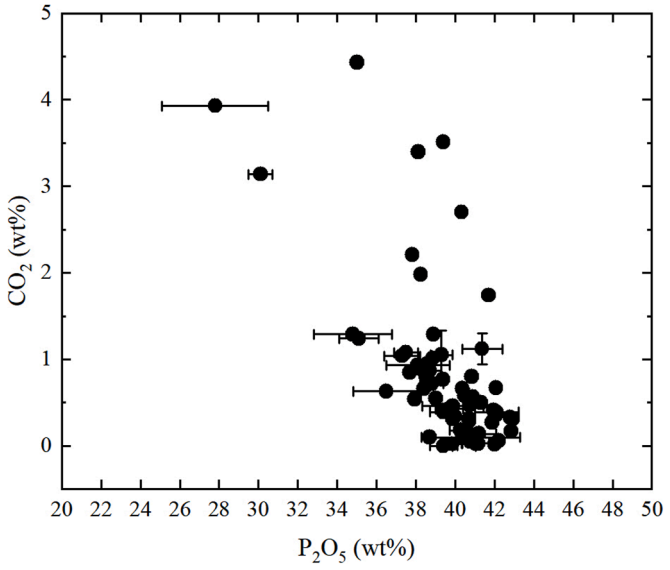

Fig. 1. CO_2 contents of common geological apatites determined by various techniques. Data sources: Deer et al. (1962, 1992), Gulbrandsen et al. (1966), Bhatnagar (1967), Brophy and Nash (1968), Young et al. (1969), Filipishin et al. (1981), Sommerauer and Katz-Lehnert (1985), Binder and Troll (1989), Santos and Clayton (1995), O'Reilly and Griffin (2000), Clark et al. (2016), Hammerli et al. (2021), and Wang et al. (2024).

F–OH–Cl volatiles in the *c*-axis channel (type A carbonate ions) or substituting for the PO_4 tetrahedra (type B carbonate ions) (e.g., Fleet and Liu, 2007, 2008a, 2008b). Because C usually interacts with H and O to form C–H–O fluids which strongly affect a wide spectrum of geological processes like differentiation of early Earth, partial melting of Earth's mantle, deposition of ore bodies, and regulating the habitability of the Earth (Liu et al., 2006; Hirschmann, 2016; Niu and Jiang, 2022; Xu, 2024), its abundances in apatites from different terrestrial rocks are commonly obtained by various analytical techniques (e.g., Gulbrandsen et al., 1966; Le Bas and Handley, 1979; Sommerauer and Katz-Lehnert, 1985; Santos and Clayton, 1995; Nadeau et al., 1999; Marks et al., 2012; Grunenwald et al., 2014). Opposite to this practice, its abundances in apatites from extraterrestrial rocks are usually undetermined though (McCubbin et al., 2015).

This dichotomy phenomenon is mainly due to the interplay of analytical methods and availability of apatite samples. For the terrestrial apatites like that from Durango, Mexico (Young et al., 1969), a large amount of well-separated material is usually not a problem, so that bulk analyses can be readily performed to obtain the CO_2 content (Table 1; the content of the carbonate ion in apatite is hereafter referred to as the amount of CO_2 in wt% or wt ppm). As to the extraterrestrial apatites, a few tiny grains with the sizes of several or several tens of micrometers may be fortuitously found in precious but limited meteorites or specimens returned by spacecrafts (Boyce et al., 2010; McCubbin et al., 2010). Obviously, bulk analyses are unfavorable even when they are not entirely impossible.

In situ microanalyses can play significant roles in quantifying the CO_2 contents in both the terrestrial apatites and the extraterrestrial apatites. Via stoichiometric calculations based on P + Si + S + C = 3 (i.e., type B carbonate), electron probe microanalysis (EPMA) was sometimes used to constrain the CO_2 contents (e.g., Le Bas and Handley, 1979; Sommerauer and Katz-Lehnert, 1985; Comodi and Liu, 2000). As C may enter the *c*-axis channel (type A carbonate), this by-difference technique bears substantial uncertainty. Another in situ method used to obtain the CO_2 content in apatites is secondary ionization mass spectrometry (SIMS; Riker et al., 2018; Li et al., 2021), which requires prohibitively expensive instrument, currently works well likely for CO_2-rich apatites only (with CO_2 content probably not less than ~1000 wt ppm; Boyce et al., 2010; Riker et al., 2018; Li et al., 2021), and is thus not widely used. A third in situ method, nuclear reaction analysis (NRA), has similar difficulties like the SIMS has (e.g., a high detection limit of ~1130 wt ppm CO_2; Clark et al., 2016) and is similarly rarely used. Utilizing the strong infrared (IR) signals of the carbonate ions in apatites (particularly, the asymmetric stretching vibrations v_3 from ~1300 to 1600 cm^{-1}; Elliott, 1994; Fleet and Liu, 2007, 2008a, 2008b; Tacker, 2008; Fleet, 2017), a fourth in situ method, Fourier transform infrared spectroscopy (FTIR), was recently developed by Clark et al. (2016; polarized transmission FTIR performed on apatite wafers polished on both sides) and by Hammerli et al. (2021; ATR-FTIR collected from polished apatite grains in rock samples like conventional petrographic thin sections). This is a very promising technique for quantifying CO_2 in apatites, considering the wide availability of the instrument, the low cost of the analysis, and the low detection

Table 1
Key sample information and analytical details, and CO_2 content (wt ppm) of Durango apatites.

Analysis #[a]	Sample features	Method or instrument	CO_2 content
1	Powder crushed from many crystals	Gasometric method	500
2	Powder ground from many crystals	C–S automatic IR analyzer	300 (15)[b]
3	Powder CDA1 ground from one crystal	C Element analyzer	455 (22)
4	Powder CDA2 ground from one crystal	C Element analyzer	242 (4)
5	Powder admixed with KBr	Unpolarized FTIR analyses	337 (103)
6	Thin sections made from one crystal	Polarized FTIR analyses	280 (120)
7	Thin sections made from one crystal	Polarized FTIR analyses	227 (10)

[a] 1 from Young et al. (1969), 2 from Binder and Troll. (1989), 3 from Peck and Tumpane (2007), 4 from Peck and Tumpane (2007), 5 from Marks et al. (2012), 6 from Clarks et al. (2016), 7 from Wang et al. (2024).
[b] Number in the parentheses representing one standard deviation; 300 (15) read as 300 ± 15.

limit (a few wt ppm CO_2; Clark et al., 2016). However, there are still some shortcomings in this method, which prevent its wide application: in the former case, the apatite crystals have to be relatively large and crystallographically oriented in order to perform the required polarized FTIR analyses (Clark et al., 2016); in the latter case, it has to be specifically calibrated for the ATR crystal used, and works well only for relatively high CO_2 conditions because of the much weaker IR signals thus-collected (~100 wt ppm; Hammerli et al., 2021).

In this study, we experimentally demonstrate that unpolarized transmission FTIR analyses acquired from unoriented apatite grains can be used to accurately constrain the CO_2 content as long as a large number of analyses can be accomplished. Our further calculations show that as the number of the analyses increases, the accuracy of the result improves quickly and significantly. For common geological applications, three or four unpolarized transmission FTIR analyses collected from random unoriented apatite grains are enough for a satisfactory CO_2 determination.

2. Unpolarized transmission FTIR experiments

A yellowish gem-quality apatite crystal (~18 mm in diameter and ~10 mm long) from Durango, Mexico was used in our FTIR experiments; some fractions of this crystal were employed in the experiments of Li et al. (2020), with extensive compositional data reported. The apatites from the region Durango have been geologically, mineralogically, compositionally and spectroscopically well characterized (e.g., Young et al., 1969; Levitt and Condrate, 1970; Hughes et al., 1989; McDowell et al., 2005; Wang et al., 2024). Due to their excellent intragranular and intergranular compositional homogeneity, Durango apatites have been widely used as reference materials for some major elements, trace elements and volatiles in EPMA analysis, SIMS analysis, laser-ablation inductively coupled plasma mass spectrometry analysis, etc (e.g., Boyce et al., 2010; Chew et al., 2016; Riker et al., 2018; Li et al., 2021; Hu et al., 2021; Chen et al., 2024). Their chemical formula is generally $Ca_{9.83}Na_{0.08}Sr_{0.01}REE_{0.09}(PO_4)_{5.87}(SO_4)_{0.05}(SiO_4)_{0.06}(AsO_4)_{0.01}(CO_3)_{0.01}F_{1.90}Cl_{0.12}(OH)_{0.01}$ (Young et al., 1969), and their CO_2 content is approximately 227–500 wt ppm (Young et al., 1969; Wang et al., 2024; see later discussion).

Our apatite crystal was almost clear and transparent, but it did contain some tiny inclusions, as similarly observed for Durango apatites by Wang et al. (2011) and Gu and Pei (2024). Thanks to the poorly developed cleavages in apatites (Deer et al., 1992), this crystal was gently crushed to generate random fragments from which 20 small fragments without discernible inclusions were arbitrarily hand-picked under optical microscope, mounted on glass slides with crystalbond, and reduced to desired thickness by manually grinding and polishing on both sides under water with a series of SiC abrasive papers. Eventually, the polished thin sections were removed from the glass slides, immersed in acetone for 30 min to dissolve the crystalbond, soaked in ethanol for another 30 min, dried at ~110 °C in an oven for several hours, and then analyzed with an FTIR spectroscope. The thicknesses of the thin sections, ranging from ~53 to 99 μm, were measured with a digital micrometer (accuracy ± 2 μm). The crystallographic orientations of the thin sections were unknown.

Unpolarized transmission FTIR measurements were conducted at room temperature using a Nicolet iN10 MX IR Microscope (He et al., 2019; Yan et al., 2023). The instrument was equipped with a high-energy Ever-Glo infrared source, a standard KBr beam splitter, a liquid-nitrogen-cooled MCT detector. Some key analytical conditions were a data range of 675–4000 cm^{-1}, an aperture size of 50 × 50 μm^2, a resolution of 4 cm^{-1}, and 512 scans for every analysis. In every IR analysis, the background was analyzed first, and the sample was analyzed subsequently. The IR spectra were processed by using the PeakFit V4.12 software (SPSS Inc.).

3. Results and discussions

As knowing the CO_2 content of Durango apatites is a prerequisite to the success of this study, we first summarize all previous measurements to establish a reference CO_2 content. Next we present the results from the unpolarized transmission FTIR experiments, and demonstrate that the reference CO_2 content has been well reproduced. Then we report the result from some simple calculations to show the correlation between the number of the FTIR analyses and the accuracy of the CO_2 determination. Finally, we have simple discussions on some relevant issues.

3.1. CO_2 content of Durango apatites: a reference value

The CO_2 content of Durango apatites has been measured for seven times using a number of analytical techniques, varying from 227 (10) to 500 wt ppm (Table 1; Young et al., 1969; Binder and Troll, 1989; Peck and Tumpane, 2007; Marks et al., 2012; Clark et al., 2016; Wang et al., 2024). Since Durango apatites sometimes contain micro inclusions of different types (pure liquid inclusions, gas–liquid inclusions, multiphase inclusions with daughter minerals like anhydrite and barite, and solid inclusions; Gu and Pei, 2024), the bulk analyses conducted on powdered samples might have generated relatively low and likely appropriate CO_2 contents in some cases (e.g., analyses 2, 4 and 5 in Table 1), but yielded significantly overestimated CO_2 contents in other cases (e.g., analyses 1 and 3 in Table 1). In contrast, in situ micro IR analyses carried out on well-polished thin sections made from clear Durango apatite single crystals, with their extraordinary power in identifying and hence removing the influence of potential contaminant inclusions, might have highly possibly led to generally accurate CO_2 contents (e.g., analyses 6 and 7 in Table 1). It is remarkable that those relatively low CO_2 contents from some of the bulk analyses closely match the values suggested by the in situ micro IR analyses, as shown in Fig. 2.

Excluding the two large CO_2 values from the bulk analyses (the red circles in Fig. 2), we have derived from the rest five analyses a CO_2 content of 277 (44) wt ppm for Durango apatites. This value is hereafter treated as our reference CO_2

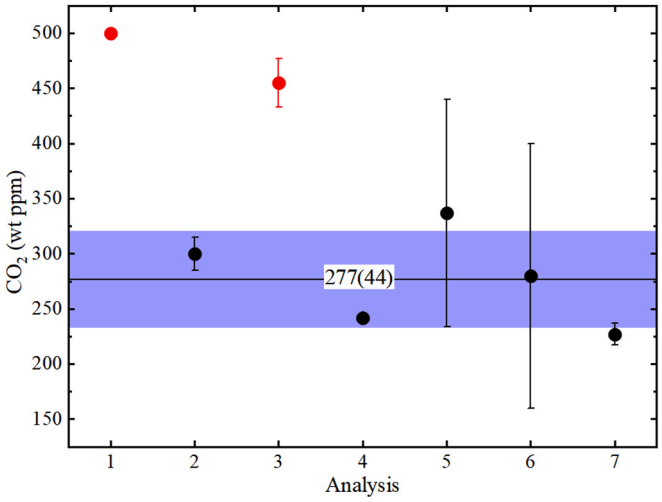

Fig. 2. CO_2 contents of Durango apatites constrained by different analyses from different studies (as listed in Table 1). For key sample information and analytical features, see Table 1. The horizontal light blue band represents our reference value, 277 (44) wt ppm CO_2, calculated from the five analyses represented by the black circles.

content, and is used to examine the feasibility of our new analytical method.

3.2. CO_2 content of Durango apatites: result from unpolarized transmission FTIR spectra

Fig. 3 illustrates the IR spectra (from 1300 to 1700 cm^{-1}) after being corrected for their baseines. 17 of the spectra do not contain detectable signals of inclusions, display IR features for carbonates in apatites well in agreement with early studies (Fleet and Liu, 2008a; Tacker, 2008; Clark et al., 2016; Hammerli et al., 2021; Wang et al., 2024), and are thus used to establish our new analytical method.

IR spectra taken from crystals with different crystallographic orientations usually have variable and curved baselines, and a unanimously applicable baseline-correction procedure is important. Previously, Clark et al. (2016) was able to simulate the baseline of their polarized IR spectra of apatites by drawing a tangent line through the lowest point on either side of the asymmetric stretching vibrational bands v_3 in the region of 1300–1600 cm^{-1} (the tangent line method). As we have found out and shown in Fig. 4 (the red line), this method does not always work in the cases of our unpolarized IR spectra. Wang et al. (2024) used the concave rubber band algorithm to model the baseline of their IR data in the range of 400–4000 cm^{-1}. Since the local lowest points of our unpolarized IR spectra in the region of 1300–1600 cm^{-1} often appear at different wavenumbers, the application of this algorithm should result in fluctuations in the baseline correction process. Here we have adopted an algorithm, the "Best-fit" function embedded in the PeakFit V4.12 software, which works in all our cases, to make the baseline corrections (the broken green curve in Fig. 4). Compared to the tangent line method and the concave rubber band algorithm, our baseline

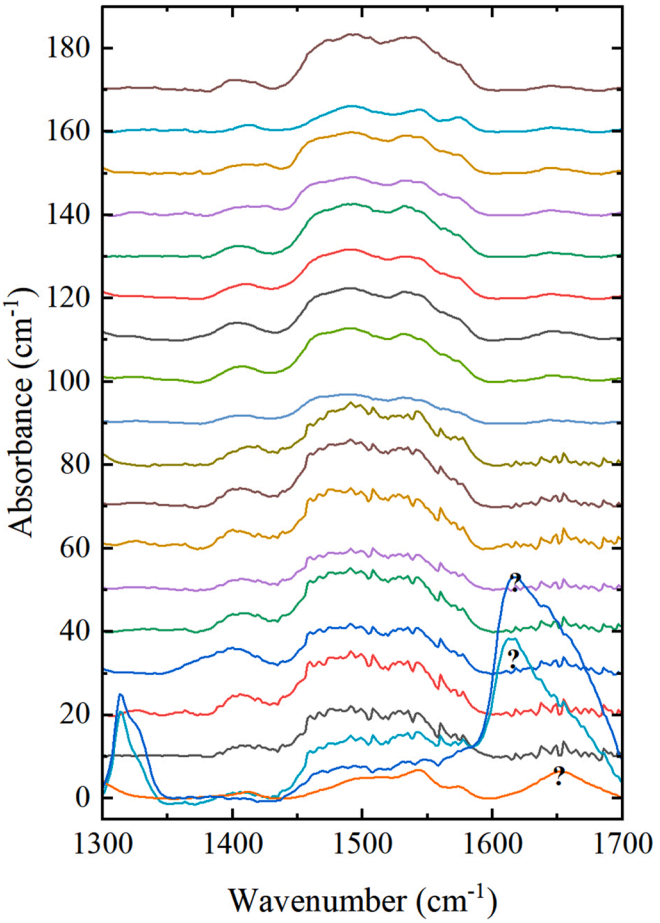

Fig. 3. Baseline-corrected IR spectra (1300-1700 cm^{-1}). Note that three spectra, denoted by question marks, likely contain signals of unknown inclusions. They are excluded from our discussions hereafter.

correction procedure clearly leads to inevitable overestimates on the integrated absorbances (A).

By employing the method of Clark et al. (2016), the CO_2 concentration (C; wt ppm) can be calculated,

$$C = \alpha A_{total}/d,$$

where A_{total} is the total integrated absorbance in the wavenumber region of 1300–1600 cm^{-1}, d is the sample thickness (cm), and α is a constant with the value of 0.0756 (36) wt ppm·cm^2. With IR measures performed using polarized light, the total integrated absorbance can be obtained as $A_{total} = A_{E//c} + 2A_{E\perp c}$ (Clark et al., 2016); $A_{E//c}$ and $A_{E\perp c}$ stand for the integrated absorbance for the condition of light E vector parallel to the c-axis ($E//c$) and perpendicular to the c-axis ($E\perp c$), respectively. In our cases with unpolarized light, A_{total} can be approximated as $A_{total} = 3A$ (Sambridge et al., 2008; Kovács et al., 2008; Withers, 2013; Yan et al., 2021).

Our experimental results are summarized in Table 2. Primarily due to the effect of different crystallographic orientations, the A_{total} varies by a factor of ~2.8 (1), from ~1845 (39) to 5208 (198) cm^{-2}. Since carbonates in apatites have a small degree of anisotropy, $A_{E//c}$: $A_{E\perp c}$ = ~0.47–2.73 (Clark et al.,

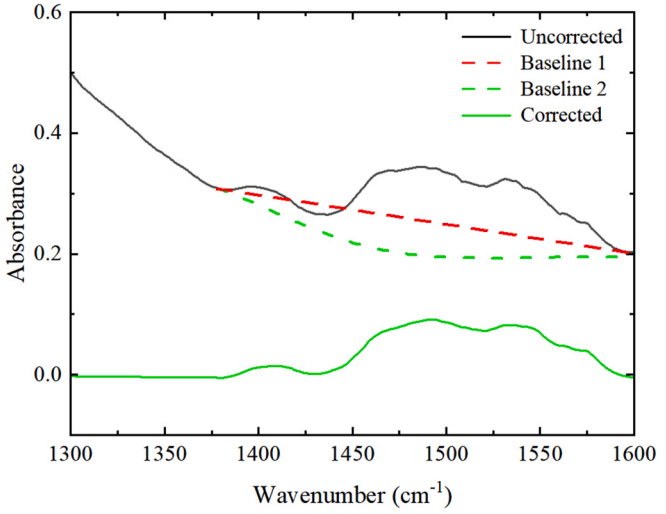

Fig. 4. Example of baseline correction for the IR data range of 1300–1600 cm^{-1} (Thickness of thin section: 83 μm). Baseline 1 is a two-point tangent line conventionally drawn through the lowest points on either side of the IR bands, and was used by Clark et al. (2016). Baseline 2 is created by the Best-fit function in the PeakFit V4.12 software, and has been adopted in this study. Note that different baseline correction schemes can lead to significant variation in the total integrated absorbances. Applying our baseline-correction procedure (i.e., Baseline 2), the concave rubber band algorithm (Wang et al., 2024; unshown here), and the two-point tangent line method (i.e., Baseline 1) to the IR spectrum shown here, we obtain A = ~1675 cm^{-2}, 1079 cm^{-2}, and 801 cm^{-2}, respectively.

Table 2
IR experimental results.

IR #	d (cm)	A (cm^{-2})[b]	A_{total} (cm^{-2})[c]	C (wt ppm)[d]	A.R.D.[e]
1	0.0055 (2)[a]	1345 (49)	4035 (147)	305 (18)	10.1 %
2	0.0053 (2)	1736 (66)	5208 (198)	394 (24)	42.2 %
3	0.0091 (2)	1352 (30)	4056 (90)	307 (16)	10.8 %
4	0.0076 (2)	1632 (43)	4896 (129)	370 (20)	33.6 %
5	0.0089 (2)	1112 (25)	3336 (75)	252 (13)	9.0 %
6	0.0060 (2)	1600 (53)	4800 (159)	363 (21)	31.0 %
7	0.0091 (2)	1736 (38)	5208 (114)	394 (21)	42.2 %
8	0.0081 (2)	1407 (35)	4221 (105)	319 (17)	15.2 %
9	0.0091 (2)	692 (15)	2076 (45)	157 (8)	43.3 %
10	0.0099 (2)	1404 (28)	4212 (84)	318 (16)	14.8 %
11	0.0083 (2)	1675 (40)	5025 (120)	380 (20)	37.2 %
12	0.0093 (2)	1140 (25)	3420 (75)	259 (14)	6.5 %
13	0.0098 (2)	1567 (35)	4701 (105)	355 (19)	28.2 %
14	0.0085 (2)	1071 (25)	3213 (75)	243 (13)	12.3 %
15	0.0074 (2)	1149 (31)	3447 (93)	261 (14)	5.8 %
16	0.0096 (2)	615 (13)	1845 (39)	139 (7)	49.8 %
17	0.0091 (2)	1516 (33)	4548 (99)	344 (18)	24.2 %

[a] Number in the parentheses representing one standard deviation; 0.0055 (2) should be read as 0.0055 ± 0.0002.
[b] A represents the integrated absorption area for the unpolarized spectrum in the range of 1300–1600 cm^{-1}.
[c] $A_{total} = 3A$.
[d] CO_2 content.
[e] Absolute Relative Difference between our CO_2 content and the reference value of 277 (44) wt ppm.

2016), this implies that our sample-preparation process was indeed random, and our dataset practically covers a wide range of different crystallographic orientations. According to Yan et al. (2021), a random sampling with a large coverage of

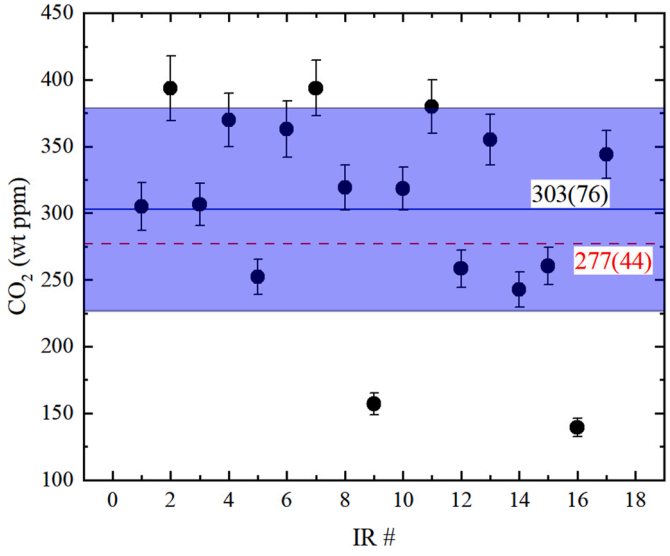

Fig. 5. CO_2 content from unpolarized transmission FTIR analyses. For the purpose of comparison, the reference CO_2 content (277 (44) wt ppm) for Durango apatite is also shown.

different orientations is key to the success in applying the unpolarized IR method to quantify anisotropically distributed species like CO_2 here in this study. Furthermore, the averaged A_{total} is 4015 (1011) cm^{-2}, indeed higher than the results reported by Clark et al. (2016; 3234 cm^{-2}) and Wang et al. (2024; ~3003 cm^{-2}), which can be readily attributed to the difference in the baseline correction procedures (Fig. 4).

The CO_2 contents are shown in Fig. 5. They vary from ~139 to ~394 wt ppm, with absolute relative differences (A.R.D.) ranging from ~5.8 % to 49.8 % when compared to the reference CO_2 content 277 (44) wt ppm. Their averaged value, 303 (76) wt ppm, is just ~9 % higher than the reference CO_2 content, in other words, the former well reproduces the latter. In addition, 12 out of the 17 CO_2 contents (~71 %) fall within one standard deviation of the mean (from 227 to 379 wt ppm; Fig. 5), and 16 (~94 %) place within two standard deviations (from 151 to 455 wt ppm; Table 2), indicating an almost normal distribution.

3.3. Quantifying CO_2 in apatites using multiple unpolarized transmission FTIR analyses

Efforts have been made to assess the feasibility of using multiple unpolarized transmission FTIR analyses to quantify anisotropically distributed water in nominally anhydrous minerals (NAMs) such as olivine, orthopyroxene, clinopyroxene, and coesite (Sambridge et al., 2008; Kovács et al., 2008; Withers, 2013; Qiu et al., 2018; Yan et al., 2021). The present wisdoms are that two analyses from randomly oriented grains may yield a result with a relative difference (R.D.) < ±25 % to the true value, and 10 or more analyses may lead to a result with a R.D. < ±10 % (Qiu et al., 2018). Little has been done to evaluate the potentials of applying multiple unpolarized transmission FTIR analyses to quantify IR-absorbing volatiles in volatile-bearing minerals like apatite,

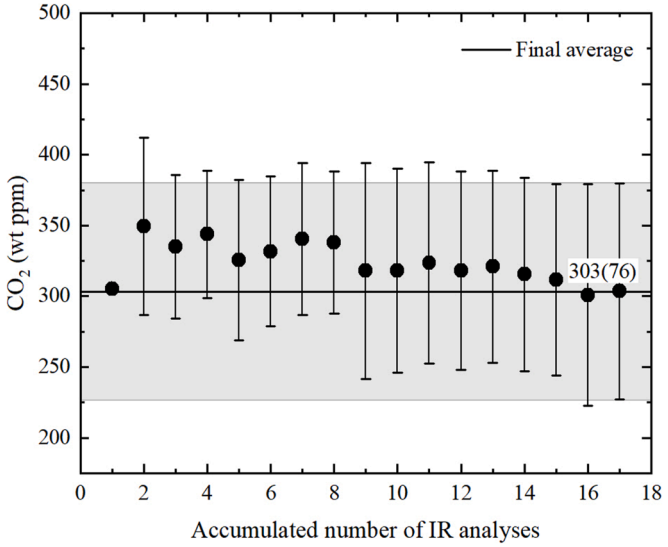

Fig. 6. Variation between CO_2 content and accumulated number of the IR analyses for the analysis-numbering sequence listed in Table 2.

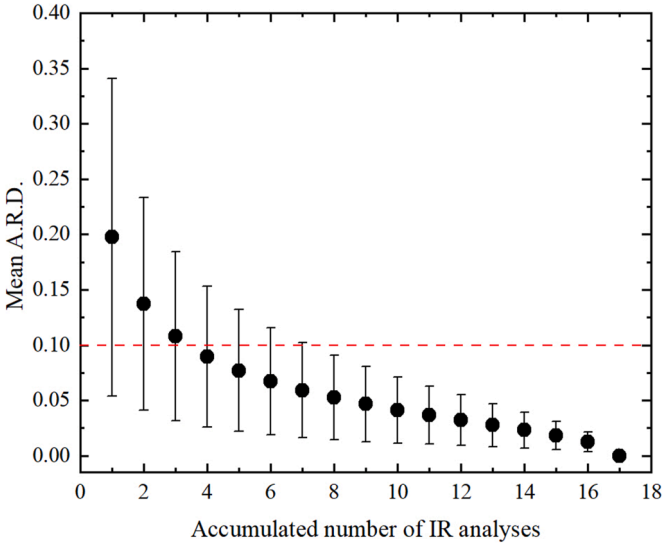

Fig. 7. Variation between Mean A.R.D. and accumulated number of the IR analyses for the one million arrangements radomly selected from 17! different arrangements defined by our 17 IR analyses. The red line, standing for an A.R.D. of 10 % and implying a generally good accuray in IR measurement, is shown for the purpose of better illustration only.

amphibole, mica, etc., which likely have more anisotropically distributing volatiles than water in the NAMs. With the experimental dataset reported in this study, it is truly a privilege to find out what is the required minimum number of the unpolarized transmission FTIR analyses from randomly oriented grains in order to constrain the CO_2 content in apatites to certain degrees of accuracy.

For the particular sequence of our 17 unpolarized transmission FTIR analyses listed in Table 2, we have calculated the CO_2 contents constrained by different accumulated numbers of the IR analyses. The result is shown in Fig. 6. Interestingly, Fig. 6 suggests that any accumulated number of the IR analyses, from 1 to 17, can lead to a CO_2 content falling within one standard deviation of the mean (from 227 to 379 wt ppm). How attractive it may be, this phenomenon is likely correct only for that particular analysis-numbering sequence listed in Table 2.

There are 17! different ways (i.e., 355 687 428 096 000) to arrange our 17 unpolarized transmission FTIR analyses. Since it is very time-consuming to carry out a full evaluation for all these arrangements, we randomly selected one million of them to examine by employing a Monte Carlo sampling method. We then calculated for each selected arrangement the A.R.D. at all accumulated numbers (from 1 to 17) of the IR analyses, and averaged the values of all A.R.D. and computed their one standard deviation at every accumulated IR analysis number obtained for all selected one million arrangements. The result is shown in Fig. 7. Fig. 7 suggests that as the accumulated number of the IR analyses increases, the A.R.D. of the result nonlinearly decreases, being very fast at the first few analyses and much slow afterwards. This phenomenon implies that there can be different minimum numbers of the IR analyses to meet different degrees of accuracy required by different studies. On the basis of a normal distribution model, specifically, one unpolarized transmission FTIR analysis mostly yields an unacceptable result with a 68 % possibility to attain a R.D. < ~34 %, and with a 95 % chance to attain a R.D. < ~48 %. In contrast, two analyses may generate a more-or-less accurate result with a 68 % possibility to attain a R.D. < ~23 % and a 95 % chance to attain a R.D. < ~33 %. Derived from three analyses, the result has a 68 % possibility to attain a R.D. < ~18 % and a 95 % chance to attain a R.D. < ~26 %, and is thus accurate enough for most studies. In more demanding cases, more analyses like 4 or 5 should be performed: in the former, the result has a 68 % possibility to attain a R.D. < ~15 % and a 95 % chance to attain a R.D. < ~22 %; in the latter, it has a 68 % possibility to attain a R.D. < ~13 % and a 95 % chance to attain a R.D. < ~19 %. If 10 analyses can be accomplished, the result should have a 68 % possibility to attain a R.D. < ~7 % and a 95 % chance to attain a R.D. < ~10 %, and is thus exceedingly accurate. More analyses are deemed as unnecessary because uncertainties introduced by other influencing factors may dominate then.

Last, we must emphasize that all these conclusions from Fig. 7 hold only if the apatite grains are fully randomly oriented. Any non-randomness will impair the accuracy somewhat, as discussed by Yan et al. (2021).

3.4. Discussions

With many different volatile components like F, OH, Cl and C in its structure, apatite plays a special role in studying the origins and evolutions of the planets and their moons in the Solar System (Nadeau et al., 1999; Greenwood et al., 2008; Boyce et al., 2010; McCubbin et al., 2010; Hu et al., 2014, 2021; Shang et al., 2022; Ge et al., 2024; He et al., 2025). Interaction between the apatites and fluids/magmas should have led to critical compositional characteristics, especially the

species, abundances and evolutions of the volatiles, registered by the apatites (Li and Hermann, 2017; Riker et al., 2018; Li et al., 2023). Accurate quantification of the volatiles, with C included, is thus very important in disclosing the chemical and physical features of evolving magmas, mantle metasomatic agents, metamorphic fluids, ore-forming hydrothermal fluids, etc. Compared to EMPA, SIMS, and NRA, the method of using multiple unpolarized FTIR spectral analyses to quantify the CO_2 contents in apatites is much more user-friendly, considering the wider availability of the instrument, the lower cost of the analysis, and the lower detection limit. In addition, it can tell whether CO_2 is incorporated in the structure of apatites or present in some inclusions. In comparison to the FTIR methods established by Clark et al. (2016) and Hammerli et al. (2021), its major advantage is that no troublesome sample orientation is needed. Consequently, the method reported here has the potentials to be widely used, with a promising prospect of substantially enhancing our understanding about the fluids/magmas once prevailing on the planets and their moons.

The feasibility of quantifying CO_2 in apatites by multiple unpolarized transmission FTIR analyses can be readily understood. Unlike the one-dimensional O–H bonds, the C–O bonds of a CO_3 ion form planes and point to three different directions. Plus the high crystallographic symmetry of apatites, the C–O bonds in apatites hence distribute more or less evenly in three dimensions. As shown in Fig. 8, the polarized IR measurements in Clark et al. (2016) clearly revealed that the distribution of the CO_3 ions in apatites has a small degree of anisotropy indeed, with $A_{E\perp c}$: $A_{E//c}$ = ~0.47–2.47. Using unpolarized light, the nominal polarized IR measurements from Hammerli et al. (2021) indicated a much less prominent anisotropic distribution, with $A_{E\perp c}$: $A_{E//c}$ = 0.66–0.99.

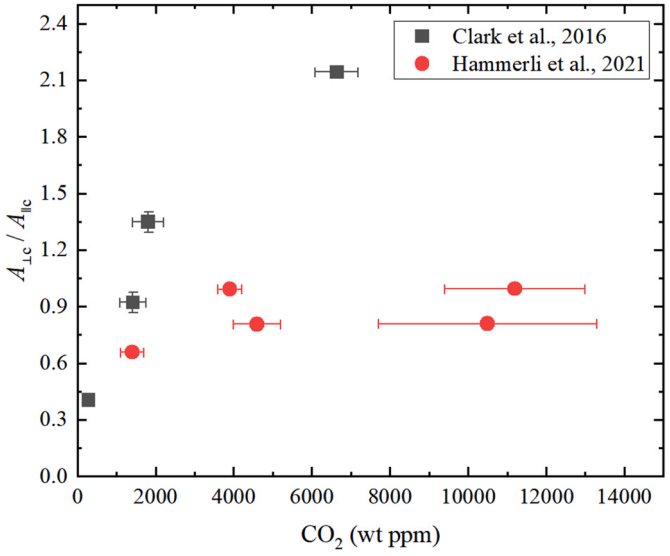

Fig. 8. Ratio of $A_{\perp c}/A_{//c}$ vs CO_2 of apatite. The IR absorbances from Clark et al. (2016) were obtained by IR measurements performed with polarized light on orientated apatite thin sections. Using unpolarized light, those from Hammerli et al. (2021) were obtained by IR measurements with the ATR alignment normal to or parallel to the *c*-axis of the apatite crystals; these IR measurements are thus "nominal" rather than conventional polarized measurements.

C may replace volatile components like F, OH, Cl and S in many other non-carbonate minerals such as sodalite, haüyne, lazurite, stilpnomelane, cancrinite, scapolite, hydrotalcite and quintinite (Deer et al., 1992; Liu et al., 2025). It is presently unclear whether our method is applicable to these minerals or not. More studies like the present one are favorable.

4. Conclusions

Determining the CO_2 content in terrestrial and extraterrestrial apatites of small grain sizes is an important issue, but has not been very easy. This study establishes a convenient method to simplify the case. By well-studied CO_2-containing Durango apatite, we have experimentally demonstrated that multiple unpolarized transmission FTIR analyses are capable to accurately quantifying the CO_2 content of apatites. Further calculations with our experimental dataset have suggested that the accuracy of the result nonlinearly increases as the number of the analyses increases. Employing the apatite-specific calibration from Clark et al. (2016; $\alpha = 0.0756$ (36) wt ppm·cm^2) and with the A_{total} approximated as $3A$, the specifics are (1) it is highly unlikely to reach a good result by conducting one analysis, (2) it is generally possible to arrive at a result with acceptable accuracy by performing two or three analyses, (3) it is almost certain to obtain a highly accurate result by collecting four or five analyses, and (4) if 10 or more analyses are possible, the accuracy can be exceedingly high (with an absolute relative difference of < ~10 %).

CRediT authorship contribution statement

Zhide Pu: Writing – original draft, Visualization, Investigation, Formal analysis, Data curation. **Zhuoran Zhang:** Investigation, Data curation. **Xinjian Bao:** Investigation, Conceptualization. **Weiran Li:** Resources, Conceptualization. **Xi Liu:** Writing – review & editing, Visualization, Validation, Supervision, Software, Resources, Project administration, Methodology, Investigation, Funding acquisition, Formal analysis, Data curation, Conceptualization.

Declaration of competing interest

The authors declare that they have no known competing financial interests or personal relationships that could have appeared to influence the work reported in this paper.

Acknowledgment

This study was financially supported by the Natural Science Foundation of China (Grant No. 42373034) and the Program of the National Mineral Rock and Fossil Specimens Resource Center from MOST, China.

References

Bhatnagar, V.M., 1967. Infra-red spectrum of an apatite from Wilberforce, Ontario, Canada. Archs. Oral Biol. 12, 429–430.

Binder, G., Troll, G., 1989. Coupled anion substitution in natural carbon-bearing apatites. Contrib. Mineral. Petrol. 101, 394–401.

Boyce, J.W., Liu, Y., Rossman, G.R., Guan, Y., Eiler, J.M., Stolper, E.M., Taylor, L.A., 2010. Lunar apatite with terrestrial volatile abundances. Nature 466, 466–469.

Brophy, G.P., Nash, J.T., 1968. Compositional, infrared, and X-ray analysis of fossil bone. Am. Mineral. 53, 445–454.

Chen, Y., Gao, J., Bi, X., Dong, S., Lei, Q., Hu, R., 2024. Simultaneous determination of the oxygen isotope ratio and volatile composition of apatite with high lateral resolution via nano-secondary-ion mass spectrometry. J. Anal. At. Spectrom. 39, 3000–3009.

Chew, D.M., Babechuk, M.G., Cogné, N., Mark, C., O'Sullivan, G.J., Henrichs, I.A., Doepke, D., McKenna, C.A., 2016. (LA,Q)-ICPMS trace-element analyses of Durango and McClure Mountain apatite and implications for making natural LA-ICPMS mineral standards. Chem. Geol. 435, 35–48.

Clark, K., Zhang, Y., Naab, F.U., 2016. Quantification of CO_2 concentration in apatite. Am. Mineral. 101, 2443–2451.

Comodi, P., Liu, Y., 2000. CO_3 substitution in apatite: further insight from new crystal-chemical data of Kasekere (Uganda) apatite. Eur. J. Mineral 12, 965–974.

Deer, W.A., Howie, R.A., Zussman, J., 1962. Rock-Forming Minerals V5. Longmans, London.

Deer, W.A., Howie, R.A., Zussman, J., 1992. An Introduction to the Rock-Forming Minerals, second ed. Prentice Hall.

Ebihara, M., Honda, M., 1987. Rare earth elements in Ca-phosphates of Allende carbonaceous chondrite. Meteoritics 22, 179–190.

Elliott, J.C., 1994. Structure and Chemistry of the Apatites and Other Calcium Orthophosphates. Elsevier, Amsterdam.

Filipshin, F.L., Mineev, D.A., Butler, A.S., Kataeva, Z.T., 1981. Monokliner chlorapatite in den magnesia-skarnen des Aldanschildes (Ostsibirien). Izw. Vyssh. Uchebn. Zavad. Geol. Ravz. 3, 1038 (in Russian, cited in Binder and Troll, 1989).

Fleet, M.E., Liu, X., 2007. Coupled substitution of type A and B carbonate in sodium-bearing apatite. Biomaterials 28, 916–926.

Fleet, M.E., Liu, X., 2008a. Accommodation of the carbonate ion in fluoapatite synthesized at high pressure. Am. Mineral. 93, 1460–1469.

Fleet, M.E., Liu, X., 2008b. Type A-B carbonate chlorapatite synthesized at high pressure. J. Solid State Chem. 181, 2494–2500.

Fleet, M.E., 2017. Infrared spectra of carbonate apatites: evidence for a connection between bone mineral and body fluids. Am. Mineral. 102, 149–157.

Ge, L., Xie, Q., Yan, J., Huang, S., Yang, L., Li, Q., Xie, J., 2024. Geochemistry of apatite from Zhuxiling tungsten deposit, eastern China: a record of magma evolution and tungsten enrichment. Solid Earth Sci. 9, 100163.

Greenwood, J.P., Itoh, S., Sakamoto, N., Vicenzi, E.P., Yurimoto, H., 2008. Hydrogen isotope evidence for loss of water from Mars through time. Geophys. Res. Lett. 35, L05203.

Grunenwald, A., Keyser, C., Sautereau, A.M., Crubezy, E., Ludes, B., Drouet, C., 2014. Revisiting carbonate quantification in apatite (bio)minerals: a validated FTIR methodology. J. Archaeol. Sci. 49, 134–141.

Gu, Y., Pei, J., 2024. Inclusion characteristics of yellow-green apatite from Mexico. J. Gems Gemmol. 26, 34–47.

Gulbrandsen, R.A., Kramer, I.R., Beatty, L.B., Mays, R.E., 1966. Carbonate-bearing apatite from Faraday Township, Ontario, Canada. Am. Mineral. 51, 819–824.

Hammerli, J., Hermann, J., Tollan, P., Naab, F., 2021. Measuring in situ CO_2 and H_2O in apatite via ATR-FTIR. Contrib. Mineral. Petrol. 176, 105.

He, H., Li, L., Hu, S., Gao, Y., Zhou, Z., Qiu, M., Zhou, D., Liu, H., Li, R., Hao, J., Hui, H., Lin, Y., 2025. Water abundance in the lunar farside mantle. Nature. https://doi.org/10.1038/s41586-025-08870-x.

He, M., Yan, W., Chang, Y., Liu, K., Liu, X., 2019. Fundamental infrared absorption features of α-quartz: an unpolarized single-crystal absorption infrared spectroscopic study. Vib. Spectrosc. 101, 52–63.

Hirschmann, M.M., 2016. Constraints on the early delivery and fractionation of Earth's major volatiles from C/H, C/N, and C/S ratios. Am. Mineral. 101, 540–553.

Hu, S., Lin, Y., Zhang, J., Hao, J., Feng, L., Xu, L., Yang, W., Yang, J., 2014. NanoSIMS analyses of apatite and melt inclusions in the GRV 020090 Martian meteorite: hydrogen isotope evidence for recent past underground hydrothermal activity on Mars. Geochim. Cosmochim. Acta 140, 321–333.

Hu, S., He, H., Ji, J., Lin, Y., Hui, H., Anand, M., Tartèse, R., Yan, Y., Hao, J., Li, R., Gu, L., Guo, Q., He, H., Ouyang, Z., 2021. A dry lunar mantle reservoir for young mare basalts of Chang'e-5. Nature 600, 49–53.

Hughes, J.M., Cameron, M., Crowley, K.D., 1989. Structural variations in natural F, OH, and Cl apatites. Am. Mineral. 74, 870–876.

Kovács, I., Hermann, J., O'Neill, H.StC., Gerald, J.F., Sambridge, M., Horváth, G., 2008. Quantitative absorbance spectroscopy with unpolarized light: Part II. Experimental evaluation and development of a protocol for quantitative analysis of mineral IR spectra. Am. Mineral. 93, 765–778.

Le Bas, M.J., Handley, C.D., 1979. Variation in apatite composition in ijolitic and carbonatitic igneous rocks. Nature 279, 54–56.

Levitt, S.R., Condrate, Sr.R.A., 1970. The polarized infrared spectra of hydroxyl ion in fluorapatite. Appl. Spectrosc. 24, 288–289.

Li, H., Hermann, J., 2017. Chlorine and fluorine partitioning between apatite and sediment melt at 2.5 GPa, 800 ^{o}C: a new experimentally derived thermodynamic model. Am. Mineral. 102, 580–594.

Li, W., Chakraborty, S., Nagashima, K., Costa, F., 2020. Multicomponent diffusion of F, Cl and OH in apatite with application to magma ascent rates. Earth Planet Sci. Lett. 550, 116545.

Li, W., Costa, F., Nagashima, K., 2021. Apatite crystals reveal melt volatile budgets and magma storage depths at Merapi volcano, Indonesia. J. Petrol. 66, egaa100.

Li, W., Costa, F., Oppenheimer, C., Nagashima, K., 2023. Volatile and trace element partitioning between apatite and alkaline melts. Contrib. Mineral. Petrol. 178, 9.

Liu, X., O'Neill, H.StC., Berry, A.J., 2006. The effects of small amounts of H_2O, CO_2 and Na_2O on the partial melting of spinel lherzolite in the system CaO-MgO-Al_2O_3-SiO_2 ± H_2O ± CO_2 ± Na_2O at 1.1 GPa. J. Petrol. 47, 409–434.

Liu, X., Sui, X., Bao, X., He, M., 2025. Fate of the last drops of serpentinizing fluid: crystallization of unusual minerals. Solid Earth Sci. 10, 100213.

Marks, M.A.W., Wenzel, T., Whitehouse, M.J., Loose, M., Zack, T., Barth, M., Worgard, L., Krasz, V., Eby, G.N., Stosnach, H., Markl, G., 2012. The volatile inventory (F, Cl, Br, S, C) of magmatic apatite: an integrated analytical approach. Chem. Geol. 291, 241–255.

McCubbin, F.M., Steele, A., Nekvasil, H., Schnieders, A., Rose, T., Fries, M., Carpenter, P.K., Jolliff, B.L., 2010. Detection of structurally bound hydroxyl in fluorapatite from Apollo Mare basalt 15058,128 using TOF-SIMS. Am. Mineral. 95, 1141–1150.

McCubbin, F.M., Vander Kaaden, K.E., Tartèse, R., Klima, R.L., Liu, Y., Mortimer, J., Barnes, J.J., Shearer, C.K., Treiman, A.H., Lawrence, D.J., Elardo, S.M., Hurley, D.M., Boyce, J.W., Anand, M., 2015. Magmatic volatiles (H, C, N, F, S, Cl) in the lunar mantle, crust, and regolith: abundances, distributions, processes, and reservoirs. Am. Mineral. 100, 1668–1707.

McDowell, F.W., McIntosh, W.C., Farley, K.A., 2005. A precise ^{40}Ar-^{39}Ar reference age for the Durango apatite (U-Th)/He and fission-track dating standard. Chem. Geol. 214, 249–263.

Nadeau, S.L., Epstein, S., Stolper, E., 1999. Hydrogen and carbon abundances and isotopic ratios in apatite from alkaline intrusive complexes, with a focus on carbonatites. Geochim. Cosmochim. Acta 63, 1837–1851.

Niu, P.-P., Jiang, S.-Y., 2022. Fluid inclusion and stable isotope (C-H-O-S) constraints on the genesis of the Heilongtan-Xiejiagou Au deposit, northern Hubei, China. Ore Geol. Rev. 144, 104841.

O'Reilly, S.Y., Griffin, W.L., 2000. Apatite in the mantle: implications for metasomatic processes and high heat production in Phanerozoic mantle. Lithos 53, 217–232.

Pan, Y., Fleet, M.E., 2002. Compositions of the apatite-group minerals: substitution mechanisms and controlling factors. Rev. Mineral. Geochem. 48, 13–49.

Peck, W.H., Tumpane, K.P., 2007. Low carbon isotope ratios in apatite: an unreliable biomarker in igneous and metamorphic rocks. Chem. Geol. 245, 305–314.

Piccoli, P.M., Candela, P.A., 2002. Apatite in igneous systems. Rev. Mineral. Geochem. 48, 255–292.

Qiu, Y., Jiang, H., Koács, I., Xia, Q.-K., Yang, X., 2018. Quantitative analysis of H-species in anisotropic minerals by unpolarized infrared spectroscopy: an experimental evaluation. Am. Mineral. 103, 1761–1769.

Riker, J., Humphreys, M.C.S., Brooker, R.A., De Hoog, J.C.M., Eim, F., 2018. First measurements of OH-C exchange and temperature-dependent partitioning of OH and halogens in the system apatite-silicate melt. Am. Mineral. 103, 260–270.

Sambridge, M., Gerald, J.F., Kovács, I., O'Neill, H.StC., Hermann, J., 2008. Quantitative absorbance spectroscopy with unpolarized light: Part I. Physical and mathematical development. Am. Mineral. 93, 751–764.

Santos, R.V., Clayton, R.N., 1995. The carbonate content in high-temperature: an analytical method applied to apatite from the Jacupiranga alkaline complex. Am. Mineral. 80, 336–344.

Shang, S., Hui, H., Yang, Y., Chen, T., 2022. Martian hydrothermal fluids recorded in the Sm-Nd isotopic systematics of apatite in regolith breccia meteorites. Earth Planet Sci. Lett. 581, 117413.

Sommerauer, J., Katz-Lehnert, K., 1985. A new partial substitution mechanism of CO_3^{2-}/CO_3OH^{3-} and SiO_4^{4-} for the PO_4^{3-} group in hydroxyapatite from the Kaiserstuhl alkaline complex (SW-Germany). Contrib. Mineral. Petrol. 91, 360–368.

Steele, I.M., Smith, J.V., 1982. Petrography and mineralogy of two basalts and olivine-pyroxene-spinel fragments in achondrite EETA79001. J. Geophys. Res. Solid Earth 87, A375–A384.

Tacker, R.C., 2008. Carbonate in igneous and metamorphic fluorapatite: two type A and two type B substitutions. Am. Mineral. 93, 168–176.

Wang, J., Yang, Y., Liu, Y., Xia, Q., 2024. Mobilities of volatiles (H, F and C) in apatite at high temperatures. Chem. Geol. 667, 122314.

Wang, K.L., Zhang, Y., Naab, F.U., 2011. Calibration for IR measurements of OH in apatite. Am. Mineral. 96, 1392–1397.

Withers, A.C., 2013. On the use of unpolarized infrared spectroscopy for quantitative analysis of absorbing species in birefringent crystals. Am. Mineral. 98, 689–697.

Xu, Y., 2024. Evolution of Earth's habitability regulated by deep earth process. Solid Earth Sci. 9, 100190.

Yan, W., Zhang, Y., Ma, Y., He, M., Zhang, L., Sun, W., Wang, C.Y., Liu, X., 2021. Water in coesite: incorporation mechanism and operation condition, solubility and P-T dependence, and contribution to water transport and coesite preservation. Geosci. Front. 12, 313–326.

Yan, W., Lv, M., Wu, D., Sun, W., Li, X., He, M., Liu, X., 2023. Water solubility in coesite at realistic temperatures of subduction zones. Chem. Geol. 625, 121412.

Young, E.J., Myers, A.T., Munson, E.L., Conklin, N.M., 1969. Mineralogy and geochemistry of fluorapatite from Cerro de Mercado, Durango, Mexico. U.S. Geol. Survey Prof. D84–D93. Paper 650-D.